

## GROUND DEMONSTRATION OF A SPINNING SOLAR SAIL DEPLOYMENT CONCEPT<sup>1</sup>

M. Salama<sup>2</sup>, C. White<sup>3</sup>, and R. Leland  
*Jet Propulsion Laboratory*  
*California Institute of Technology, Pasadena, CA 91109*

### ABSTRACT

The dynamics of spin-deployment of a sub-scale solar sail concept (2.5-micron thick mylar film, 80-cm diameter) is investigated herein experimentally in the laboratory environment. To gain insight into the practicality of the deployment scheme, a tether configuration emulating the sail film was first deployed successfully, using the same experiment design. With the exception of some handling issues, the ultra-thin mylar film was also successfully deployed without entanglement.

Design details and observations of both experiments are discussed. Additionally, results of analytical simulations to study the dynamics of tether deployment are given.

### BACKGROUND

Since the early 20<sup>th</sup> Century, solar sailing has been advocated as an efficient means of space propulsion. And although a solar sail

has yet to be flown, the practicality of the concept has been confirmed by numerous recent studies [1, 2]. Several solar sail design options have been considered in depth for a wide variety of space travel – ranging from Earth orbiting to interstellar.

Two primary solar sail design options have emerged: three-axis-stabilized square sails, and spin-stabilized sails. In the first, lightweight compressive booms emanating from a central hub are used as the primary load-carrying structural members. The compressive loads in the booms are balanced by tensioning the sail film. In the second, the dynamics of spinning induce the needed tension field in the sail, thereby providing the desired near flatness of the film. Within these two options, there are still several other distinct concepts - each having its own set of merits and challenges. In all cases, however, the solar sail must be made of large areas (several 100's m<sup>2</sup>) of ultra-light, highly reflective thin film (orders of microns), that can be packaged into

---

<sup>1</sup> Copyright © 2001 by the American Institute of Aeronautics and Astronautics, Inc. The U.S. Government has a royalty-free license to exercise all rights under the copyright claimed herein for Government purposes. All other rights are reserved by the copyright owner.

<sup>2</sup> Associate Fellow, AIAA

<sup>3</sup> Member, AIAA

small volume during launch, then deployed to the full gossamer proportions once on-orbit. The viability of such a technology is replete with practical questions and uncertainties that must be first examined by analysis, laboratory experiments, and flight tests - prior to actual flight. To this end, two significant developments were performed in the past.

First, in the early 1990's Russian investigators began a reflector technology development program that culminated in the space deployment in 1993 of a twenty-meter diameter spinning reflector, known as Znamya-2 experiment [3]. As the ground development program progressed, close interaction between theoretical work and experimental experience proved to be indispensable - eventually leading to the success of the in-space experiment. Second, in support of a proposed three-axis-stabilized sailcraft concept intended for use in a geostationary orbit, a ground test program [4] was conducted in 1999 by DLR/ESA in collaboration with JPL/NASA. The program intended to show the feasibility of manufacturing a 20m x 20m square sail using deployable lightweight booms and extremely thin sail. Functionality of deployment of the collapsible composite boom, and the ability to handle extremely thin sail film (4.0 micron PEN film) were demonstrated in simulated zero-g and ambient environmental conditions.

For spinning sailcrafts, the dynamics of sail deployment is perhaps one of the most challenging elements of their design. During deployment, the sail mass (which could easily amount to 50% of the total sailcraft mass) must undergo extreme dynamic transformations from the compact packaging to the fully deployed gossamer configuration. Thus, a stable and controllable deployment must be assured. Herein, the paper will focus on a preliminary design implementation, analysis simulation, and demonstration of a laboratory experiment dedicated to examining the deployment dynamics and stability of a sub-scale 80-cm

diameter spinning sail. The work is intended as a preliminary substantiation of a spinning sail deployment concept proposed for a NASA interstellar mission.

## SPINNING SAIL CONCEPT

The spinning sail concept under consideration was developed as part of a recent study at JPL to send a scientific probe to the heliopause and beyond [5]. The basic sail configuration for this mission (referred to as the Interstellar Probe Mission) is shown in Figure 1. It consists of six sectors, which comprise a nearly 400-m diameter, less than one-micron thin sail. Each sector is tethered to its contiguous neighbors at the perimeter, and is initially stowed into Z-folded gores wrapped around a central cylindrical hub. Initial spin-up is accomplished by first deploying three 10-m long booms to which cold gas thrusters are mounted. Once a steady spinning rate is achieved, the sail gores are released from the hub. The centrifugal acceleration then gradually unfurls the sail gores from the star shape to the ring shape with tethers attaching the sail membrane to the central hub. Pulling on the tethers will then complete deployment of the entire 400m diameter sail.

While retaining the basic deployment sequence, the following laboratory experiments are intended to explore the feasibility of the concept, with emphasis on the dynamics and stability of the deployment process. The two main differences between the Interstellar Probe deployment concept and the deployment scheme used in the experiment are:- (1) spinning is initiated by motors rather than by cold gas thrusters, and (2) the gores are made to deploy from the star shape to the sector shape - directly without having to go through the intermediate ring configuration.

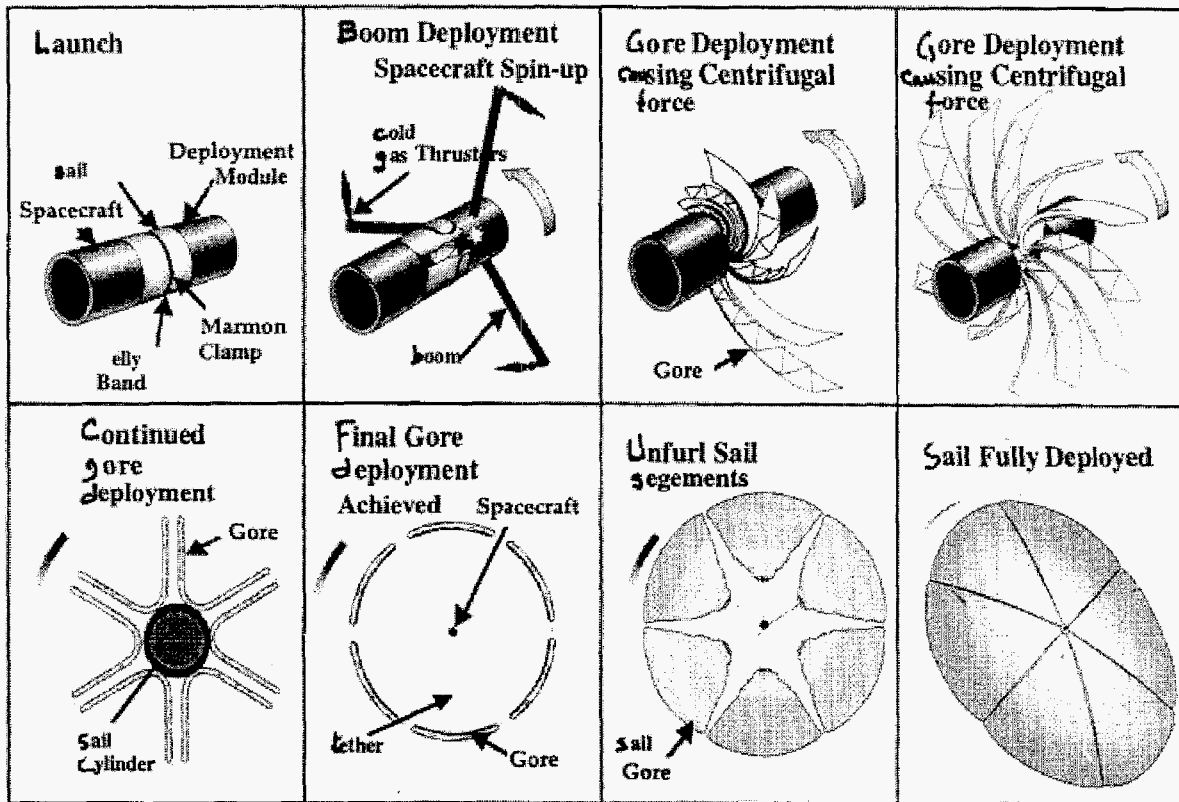


Figure 1. Deployment Concept for Interstellar Probe Mission.

### LABORATORY EXPERIMENT

With reference to Figure 1, it was envisioned that the most challenging part of the deployment would be the four steps in the lower row. This includes moving from the star configuration to the ring configuration with the sail Z-folded, followed by unrolling of the sail by pulling on the radial tethers. Within this sequence of steps, there naturally arose questions of the influence of gravity, air drag, rotation rate, radial tether release rate, and sensitivities to slight asymmetries in the experimental apparatus. To isolate and control these variables as much as possible, the deployment sequence was broken into three smaller experiments, each one increasing in complexity and culminating in the deployment of a disc-shaped sail of 2.5-micron thin film.

The first experiment used a continuous ring-shaped tether in place of the Z-folded sail membrane to demonstrate the radial release from the star configuration to the ring configuration. For the second experiment, a relatively thick 120-micron nylon film, Z-folded for stowage and reinforced along the perimeter with the tether, was used. The third experiment used a delicate 2.5-micron aluminized mylar film material, Z-folded with no perimeter tether reinforcement. All three experiments used the same hardware apparatus, shown in Figure 2. The spinning central hub consisted of two concentric, thin-walled cylindrical drums of fiberglass-fabric laminate (grade G-10), each controlled by an electric motor. The inner cylinder (5-cm diameter) serves as the drum for stowing and controlling the radial tethers. The outer cylinder, or spool, (10-cm

diameter) provides for the attachments of the sail film. As shown in the figure, the motor controlling the inner drum is mounted on the base-plate of the outer spool and made to rotate with it. Power is communicated to this motor through a slip ring assembly. The inner drum is then made to rotate very slowly with respect to the outer spool, thus allowing radial deployment and retraction of the tethers, which pass through small holes in the outer spool wall. A sail diameter of 80-cm was selected based on the diameter of the available vacuum chamber, 90-cm.

#### **a. Experiment #1 --Tether Deployment**

As mentioned, the purpose of deploying a tether from the star to ring configuration was to begin with a simplified experiment that minimizes the difficulties of handling the very fragile mylar film material. In selecting the tether material, care was taken to use rope of a reasonable mass and a sufficiently low bending stiffness. The rope tether used in the experiment had a mass of 5.5-g. Radial tethers were selected with sufficiently low mass and surface smoothness. The six radial tethers were precisely marked and cut to the same length before being attached to the central drum and fed through the holes in the outer spool. The free ends were then glued with cyanoacrylate to the ring-shaped tether at 60-degree intervals.

Spin-up and deployment to the ring configuration were accomplished on the first attempt without any difficulties. Retraction back to the star configuration was also successful. Still photographs of the steady-state configuration are shown in Figures 3 and 4. Gravitational forces caused the tether to deflect down from the horizontal plane, but it was observed that rotational rates of approximately 200 rev/min would essentially cancel these deflections.

The effect of air drag (on both the rope tether and the radial release tethers) were evident; even at steady-state, the radial tethers did not

emanate from the spool along radial lines, but rather lagged behind the spool by as much as 45-degrees. However, although gravity and air-drag effects were present, they did not limit this experiment in any significant way. The experiment was successful in showing the controlled deployment from star-to-ring configurations; the path is now open to explore the more challenging aspects of the transient dynamic stability of these deployments for the thin film sail.

#### **b. Experiments #2 & #3 --- Film Deployment**

##### Nylon Film Deployment

This next set of experiments presented the practical challenges of working with stowed and deployed thin film structures. However, experimenting first with the 120-micron nylon film eliminated a few of the challenges, while providing experience that would be valuable for the fragile 2.5-micron mylar film. The greatest benefit of the nylon lies - not so much in its greater thickness - but in its relative toughness and tear resistance.

It was decided to divide the disc-shaped sail into six 60-degree sectors. These sectors were formed by cutting a disc-shaped blank of material along radial lines from the center to outside edge, leaving a 2-cm strip of continuous material along the outside edge. This strip was then folded over the perimeter tether and sewn, thereby encasing the tether. The intention was to use the tether mass to provide extra centrifugal force to ensure full film deployment and nearly flat spinning sail. However, sewing the film created undesirable bunching-up of the nylon and introduced local film wrinkling and stiffening.

A Z-fold pattern with fold lines spaced approximately 3-cm apart was chosen for folding and stowing each sector. This gave

about 13 folds per sector. To accommodate the radial tethers, holes were punched through the film - midway between each fold line. The inside edge of the sail was simply taped to the outer spool, and the radial tethers were fed through the holes in the film, then glued to the perimeter tether. The final step of the installation process required simultaneously folding all six sectors and retracting the radial tethers to ultimately arrive at the star configuration.

Starting from the star configuration, initial spin-up and deployment of the nylon film was attempted on the bench top, but it was immediately clear that air drag would be far too large. Figure 5 captures this initial attempt in a still photo. It can be seen that in-plane shear stresses in the film (resulting from air drag) are causing the film to wrinkle and wind itself around the spool.

The experiment was then moved to the vacuum chamber and the atmosphere was evacuated to a pressure of approximately 10-Pa. Inside the vacuum chamber, the sail deployment was successful, although it was not possible to make clear photographs of this first attempt. Subsequent deployments without the perimeter tether were also successful and it was concluded that the circumferential tether was not needed. Successful deployments using estimated rotation rates as low as 100 rev/min were observed, but no attempt was made to determine a minimum rate.

#### Mylar Film Deployment

A 2.5-micron aluminized mylar film reinforced with kapton threads running in one direction was used in this test. This material had an areal density of approximately 5.1 g/m<sup>2</sup>, and an extremely low resistance to tearing - although the reinforcing did help somewhat.

Because of the rather narrow dimensions of the bulk mylar film, each of the six sectors had to be cut from the sheet separately, so that a continuous circumferential strip (if it was to be used) would have to be fabricated by adhesion. It was therefore decided to try six independent

sectors with no circumferential connections between them.

After the sectors were cut, holes were punched between each of the 13 fold lines. The sectors were carefully taped to the outer spool as before, and the radial tethers were fed through the holes. The free ends of the tethers were taped with small pieces of tape to the outer edge of the sectors. Because the sectors were independent, it was possible in this case to Z-fold each one separately, while manually controlling the radial tether by gently pulling it through the wall of the outer spool from the inside. The installation was complete once the star configuration was achieved. Details of the spool attachment are shown in Figure 6.

Deploying the 2.5-micron mylar film under 10-Pa vacuum was not the immediate success that it had been with the tether and with the nylon film. Starting from rest, the rotational speed was slowly increased to approximately 200 rev/min. The radial tethers were then activated for release, but the sail did not deploy. So, the rotational speed was increased further, and the radial motor was switched on/off numerous times. Suddenly, the sail deployed to near its full configuration. Subsequently, as the radial tethers were fully extended, the sail fully deployed. A sequence of photos - at various stages in the deployment process - were taken from the view port in the vacuum chamber. These are shown in Figure 7 - 10. The reason for the tardy deployment is still under investigation. But the leading causes may be due to binding or interference within the sectors due to excess adhesives, or due to malfunction in the motor which controls the radial tether release. Post-deployment inspection of the sail revealed tearing up to 2-cm in length in two of the six sectors, particularly near the inside edge of the sail in the vicinity of the first radial-tether hole, and at the last hole near the outside edge of the sail.

## NUMERICAL SMULATIONS

### Simulations of Tether Deployment

The dynamics of tether deployment was analyzed using DYNA3D. The tether deployment analysis was intended as a first step toward modeling the film deployment. The gravitational field and air drag were not modeled. Characteristics of the tether were chosen to match the experiment. This includes length, mass per unit length, and modulus. Rather than six tether sectors, only four, each covering a 90 degrees sector were assumed, and each was modeled with 55-elements having only uni-axial stiffness, area = 1.e-5m, and modulus = 1.e+9 N/m<sup>2</sup>. Initially, each of the four tethers is attached to the rigid cylinder at two points, then wrapped around as shown in Figure 11. At t = 0, no contact or elastic interaction is assumed between the tethers and / or the rigid cylinder.

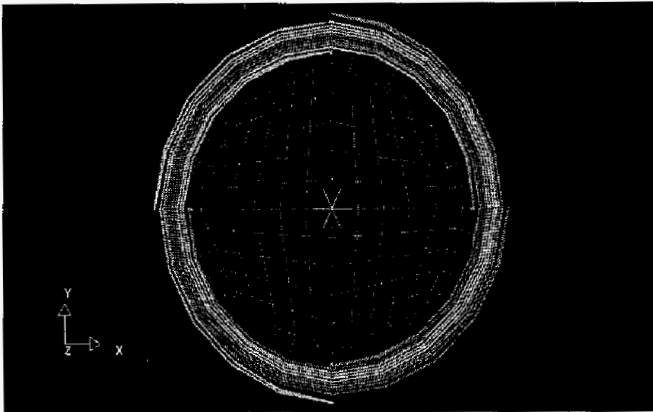


Figure 11. Four tether segments initially folded.

Deployment is accomplished in two stages, the interaction of which could be a design parameter to be selected. First is the spin-up and ensuing transient response of the tethers to the induced rotation. Spin-up is accomplished by prescribing the angular velocity,  $\omega_o(t)$ , of the central rigid cylinder such that:

$$\omega_o(t) = \begin{cases} t(\omega_{\max} / \Delta t), & 0 \leq t < \Delta t \\ \omega_{\max}, & t \geq \Delta t \end{cases} \quad (1)$$

where,  $\omega_{\max} = 120$  rpm, and  $\Delta t$  is a ramp-up time - selected parametrically from 0.01 sec to 2.0 sec.

At a prescribed time,  $t, \geq \Delta t$ , in presence of the spin-up acceleration field, the second stage of deployment is initiated by simultaneously releasing all four tethers at a prescribed rate relative to their attachment points on the rigid cylinder. Because of the centrifugal accelerations, the tethers will tend to move radially outward.

In addition to these initial and intermediate enforced motions, the tethers are also subjected to their own material damping, as well as to contact forces arising from possible interactions among each other and with the rigid cylinder. A nominal mass-proportional damping = 5% critical was assumed equally for each tether, but was later varied.

Contact interactions were modeled as follows. During a time step, if a node on the tether is within a small distance  $\epsilon_n$  from the rigid cylindrical surface, and the relative acceleration between them is negative (i.e. contact closure), the tether node is constrained to move consistently with the rigid cylinder surface. The constraint is relaxed if in a subsequent step the updated nodal accelerations indicate contact separation. On the other hand, contact between the tethers is implemented as a special case of the surface-to-surface contact [6], where equal and opposite contact forces are applied to the penetrating nodes, the magnitude of such forces is proportional to the depth of penetration. Results of the deployment analysis are summarized below for a few cases.

a. In the nominal case, the tether properties described above were used. Figure 12 shows a succession of "snap shots" (in clockwise order) of the tethers as they unfurl from the packaged state of Figure 11 to full deployment. Notice the swinging (leading

and lagging) motion of the tethers relative to the central rigid cylinder (captured in the second and third animation sketch in the top row of Figure 12). The frequency of this pendulum-like motion is a function of the tether characteristics and the rate of angular velocity. In the present case, the motion was damped out by the assumed 5% damping, and the deployment proceeded without entanglement. The last two animation sketches in the second row of Figure 12 compare very well to similar instants in the test results depicted in Figures 3 and 4.

b. Spin-up rate. In the nominal case above, a rather fast angular velocity ramp-up time  $\Delta t = 0.001$ -sec was used (a step function). In Figure 13, we compare the response time-history of a point on the outer edge of the tether between the nominal case (Figure 13a) and a more gradual spin-up,  $\omega_o(t)$ , in which  $\Delta t = 2$ -sec was used (Figure 13b). With the slow spin-up initiation rate (13b), excitation of the pendulum-like motion is no longer evident. The growth in response amplitude from 2.0 - 4.4 sec. is due to the tether radial release.

c. Effect of random variations in properties. The influence of random variability in the tether properties and geometry on their dynamics was studied in this example. Here, damping was allowed to vary randomly among the four tether segments to within  $\pm 20\%$  of the nominal 5% critical damping. The selection of damping as the single random variable was made as a simplification of the more practical but complex scenario, in which random variations could arise from various sources such as changes in properties, length, mass, cross section area, as well as damping. As can be seen from the sequence of tether motions in Figure 14, deployment did continue (clockwise order) with somewhat chaotic pendulum-like motion of the four tether segments. It is possible that such variability could have de-stabilizing effects, eventually resulting in irrecoverable entanglements.

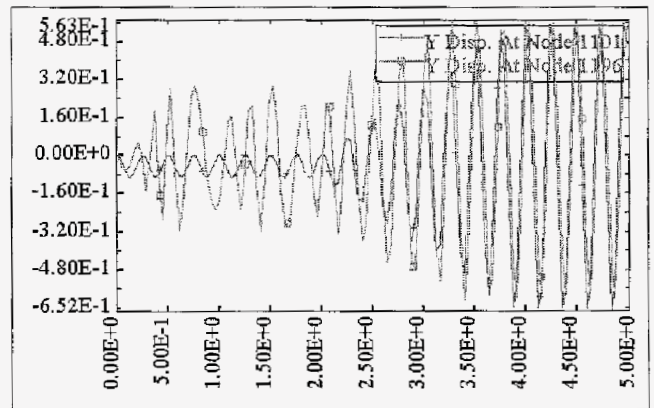


Figure 13a. Fast spin-up,  $\Delta t = 0.001$ -sec.

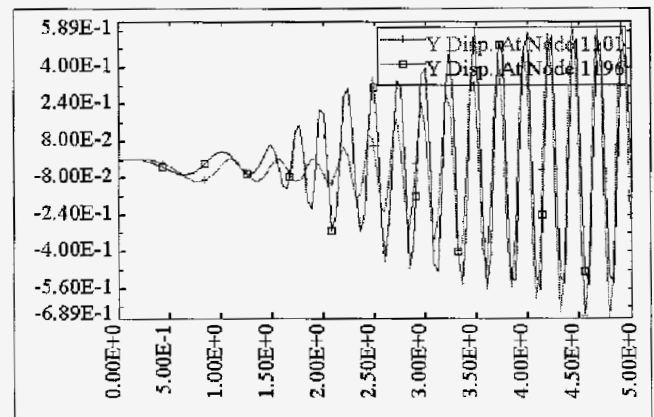


Figure 13b. Slow Spin-up,  $\Delta t = 2.0$  sec

## CONCLUSIONS

The experiments and simulations described herein were not intended as tools from which one may infer the performance of a real sail in space. Rather, they were intended to provide some hand-on experience with the extremely fragile sail film, and a basic understanding of some challenging aspects of the spin-deployment dynamics. But even in the face of the experiment limitations such as sail size, spin-up rate, and the presence of gravity, both the laboratory tests and tether simulations give strong indications that the proposed deployment scheme is quite feasible. Further experimental and analytical investigations are planned.

## ACKNOWLEDGEMENT

Funding for this research was provided by the Interstellar and Solar Sail Technology Program at JPL. The assistance of Dr. C.P. Kuo in designing the experiment setup and discussions with Dr. C. Garner are greatly appreciated.

## REFERENCES

1. McInnes, C. R., *Solar Sailing: Technology Dynamics and Mission Applications*, Springer-Verlag, London, 1999.
2. Salama, M, McInnes, C.R., and Mulligan, P., *Gossamer Sailcraft Technology, Chapter 19, Gossamer Spacecraft Membrane / Inflatable Structures Technology for Space Applications*, Editor: Jenkins, C.H., *AIAA Progress in Astronautics and Aeronautics*.
3. Melinov, M.V., and Koshelev, V.A., *Large Space Structures Formed by Centrifugal Forces*, *Earth Space Institute Series*, Gordan and Breach Science publishers, 1998.
4. Leipold, M., "ODISSEE- A Proposal for Demonstration of a Solar Sail in Earth Orbit", IAA-L98-1005, 3rd International Academy of Astronautics Conference on Low Cost Planetary Missions, Pasadena, April 1998.
5. *The Interstellar Probe Mission Architecture and Technology Report*, JPL-D-18410, October 1999, Jet Propulsion Laboratory, California Institute of technology, Pasadena, CA.
6. Hallquist, J. O., *LS-DYNA3D Theoretical Manual*, Livermore Software Technology, 1993.

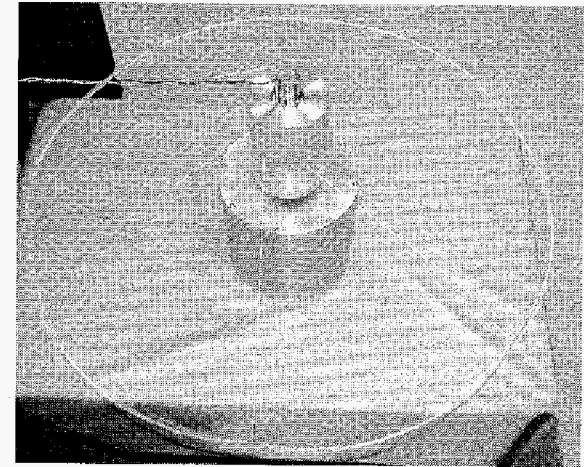
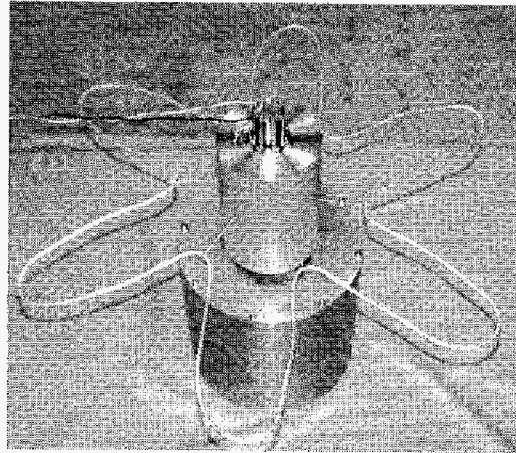
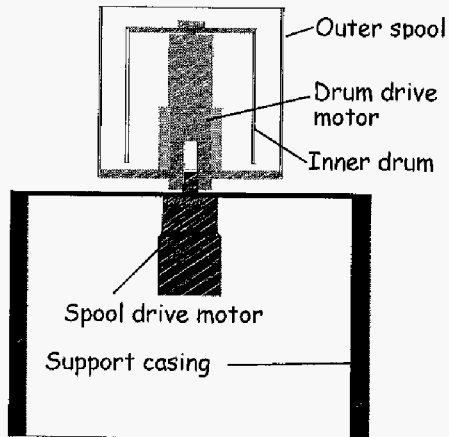


Figure 2. Spin deployment apparatus.

Figure 3. Partially deployed ring tether.

Figure 4. Fully deployed ring tether.

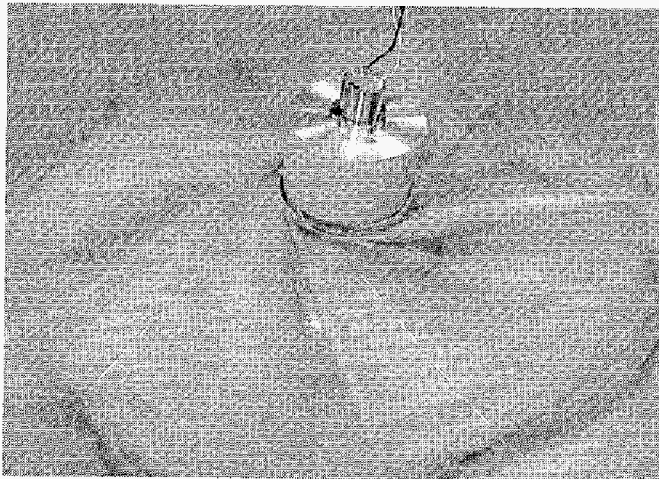


Figure 5. Initial attempt to deploy 120  $\mu$  film.

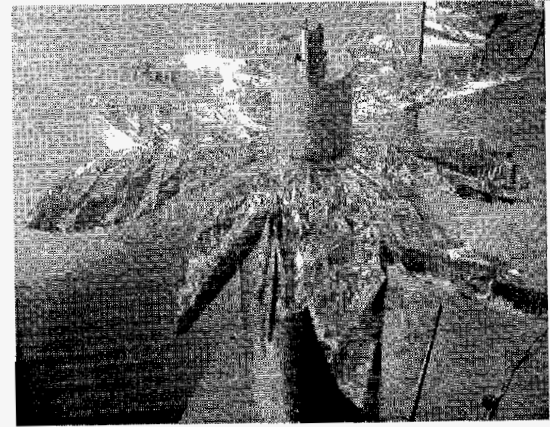
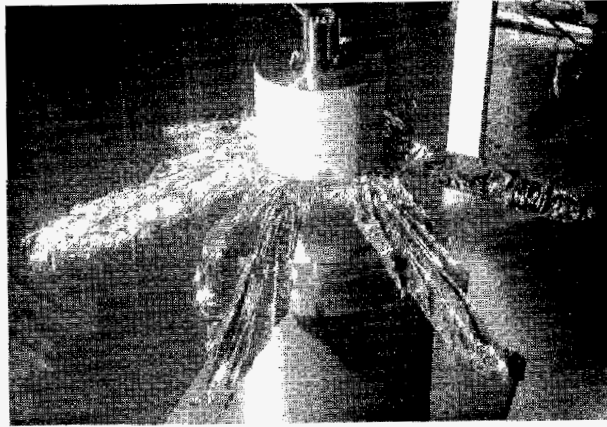
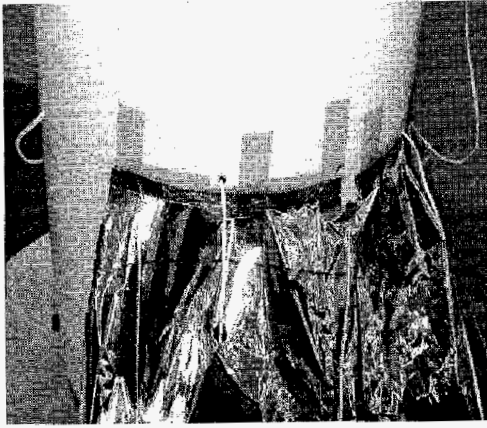


Figure 6. Film attachment to the hub.

Figure 7. Sail film before radial deployment. Figure 8. Partial deployment with binding film.

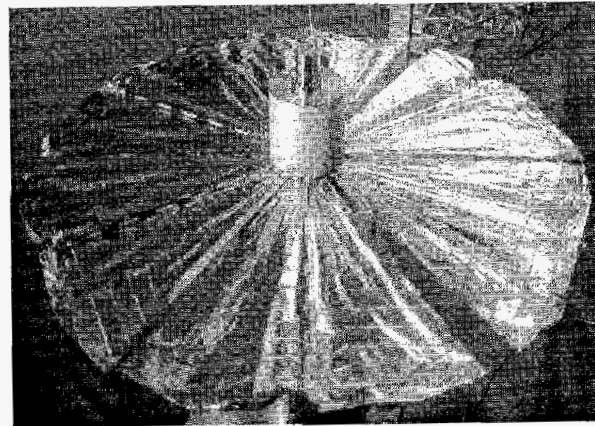
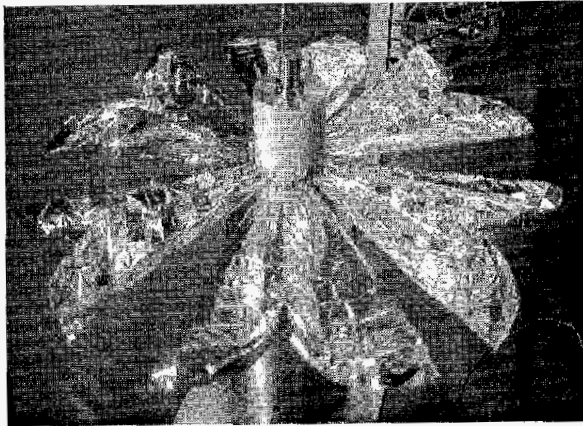
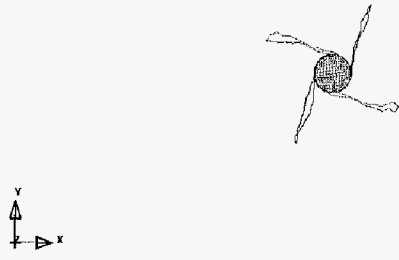
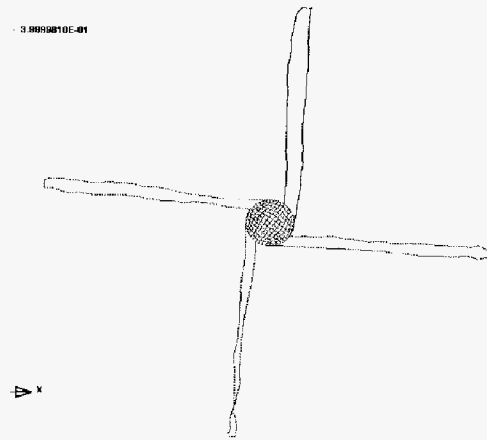


Figure 9. Partial deployment, sector extended. Figure 10. Fully deployed 2.5- $\mu$  film.

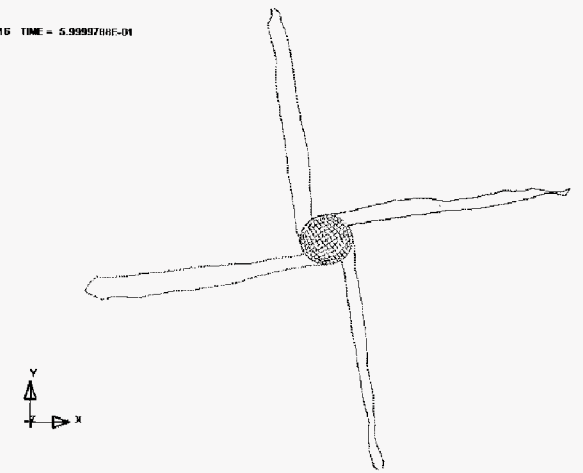
STEP 4 TIME = 1.1959795E-01



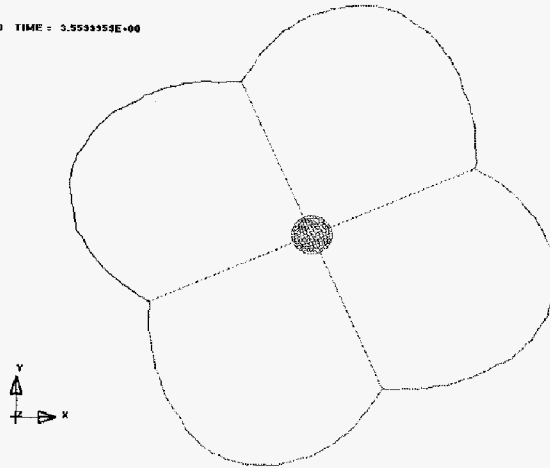
3.8869810E-01



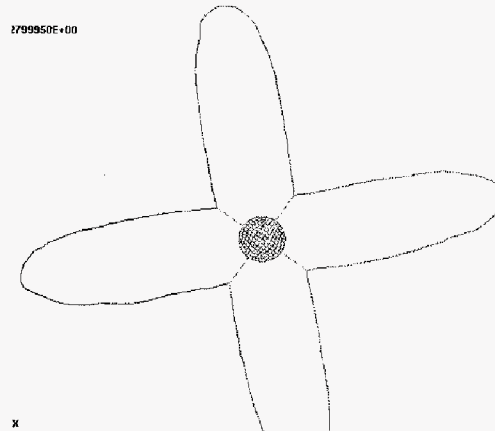
STEP 16 TIME = 5.9999788E-01



STEP 30 TIME = 3.5533553E+00



7.999950E+00



1.5809978E+00

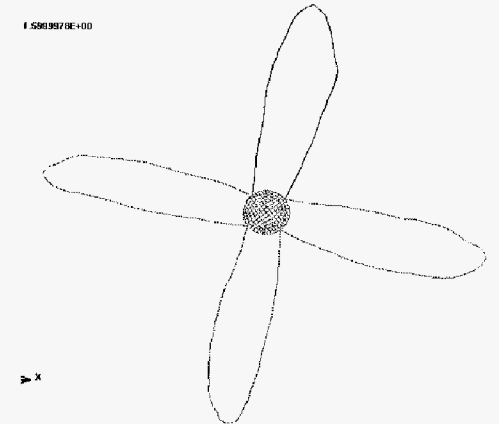


Figure 12. Simulation of tether deployment (Nominal Case).

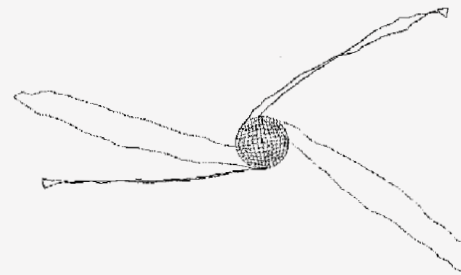
STEP 4 TIME = 1.199825E-01



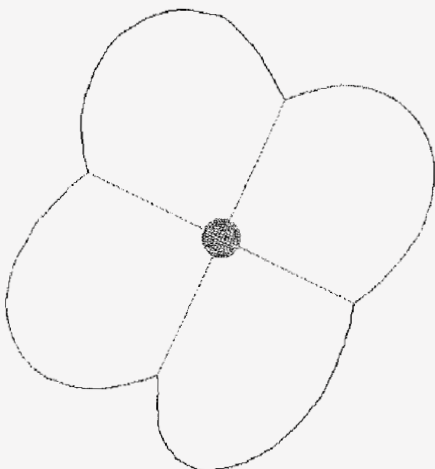
STEP 10 TIME = 3.599840E-01



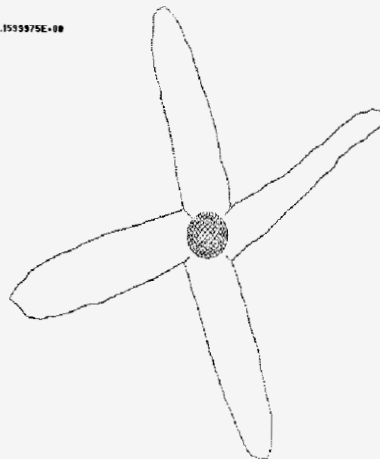
STEP 10 TIME = 5.788804E-01



STEP 04 TIME = 3.719993E+00



STEP 08 TIME = 2.155975E+00



TIME = 1.638872E+00

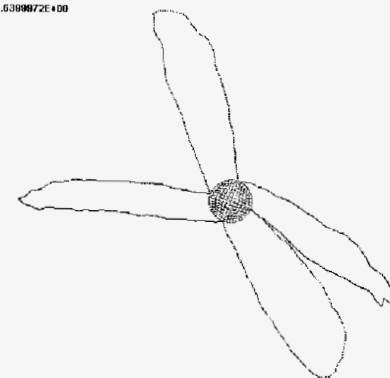


Figure 14. Effect of random variation in tether damping on deployment stability